The Effect of Heat Treatment on Microstructure and Mechanical Properties of Ti-8.5Nb-4.5Ta-13Zr Alloy

N. M. F. Mendes[2], M. W. D. Mendes[1], A. H. A. Bressiani[1], H. Takiishi[1]

[1] Nuclear and Energy Research Institute, IPEN - CNEN/SP
Av. Prof. Lineu Prestes, 2242, 05508-000, São Paulo, Brazil

[2] Federal Institute of São Paulo, IFSP
Rua Pedro Vicente, 625, 01109-010, São Paulo, Brazil

narayanna@ifsp.edu.br

Keywords: Titanium alloy, powder metallurgy, high-energy milling, heat treatment.

Abstract: The effects of the heat treatment on the phase transformations, microstructures and mechanical properties of Ti-8.5Nb-4.5Ta-13Zr alloy were studies in this work. Some of the starting powder were obtained by hydrogenation method and homogenized with metallic tantalum in a high-energy planetary mill. The samples were compacted in a uniaxial and cold isostatic presses and then, sintered at 1150 °C for 10 hours under high vacuum. The heat treatments were carried out at the same sintering temperature, above the α / β transus, at different cooling rates such as furnace cooling, air cooling and water quenching. The sintered samples were characterized using the Archimedes density method, X-ray diffraction (XRD) and scanning electron microscopy (SEM). The microhardness was measured using the Vickers indentation (ASTM E384-11 Standard). It was shown that the microstructure of Ti-8.5Nb-4.5Ta-13Zr alloy consists of beta-phase matrix and alpha-phase region of two structures: equiaxed and needle-like grains also known as Widmanstätten structure. The precipitation of the alpha-phase in the beta-phase matrix led to an increase in Vickers microhardness of the alloy which was furnace cooled. Moreover, a few remaining pores were still found and density above 98% was achieved.

Introduction

Titanium and its alloys can be used as a biomaterial, mainly because the combination of outstanding properties. Low density, high strength, low elastic modulus, high stiffness, superior biocompatibility and good corrosion resistance are some these properties [1,2]. The β-type titanium alloys have a lower modulus of elasticity compared with the alloys of the α + β and α type alloys. Research to develop the β-type alloys composed unique of biocompatible elements such as niobium, tantalum and zirconium are objects of study [3]. In titanium alloy, the niobium and tantalum are stabilization elements of the β-phase and zirconium is considered neutral element [4,5]. In addition to the stabilizing elements of phases, another feature can determine and control the final product that it is the heat treatment application. Therefore, the final microstructure of beta titanium alloy depends on the elements constituting the alloy, temperature and rate of cooling from the heat treatment [6,7].

Thus, the aim the present work was to study the microstructural behavior and mechanical property of hardness in different cooling conditions of Ti-8.5Nb-4.5Ta-13Zr alloy.

Experimental

The starting powders TiH_2, NbH and ZrH_2 were obtained from hydrogenation of plates, billets and sponge fines, respectively. The metallic tantalum powder was supplied by Aldrich Fine Chemicals. The hydrogenation was carried out under hydrogen atmosphere of 0.8 MPa at 700 °C for titanium and niobium, and at 550 °C for zirconium, for 1.5 h and 0.5 h, respectively. After the hydrogenation, these materials were comminuted and sieved in < 500 μm (35 mesh) sieve. Further, the powders were milled and homogenized in the high-energy planetary mill (Pulverisette) at

200 rpm for 240 minutes. The cyclohexane was used as organic additive for milling and afterward it was removed under vacuum. Afterwards, 6 mm diameter samples were uniaxially compacted at 65 MPa, followed by cold isostatic compaction at 200 MPa. The sintering occurred at 1150 °C for 10 h under vacuum (10^{-4} Pa) and the heat treatments were carried from the sintering temperature, above the α / β transus, with different cooling rates such furnace cooling (FC), air cooling (AC) and water quenching (WQ).

For materials characterization, the particle size distribution by laser scattering technique and the density as-sintered using Archimedes method were used. The samples were subjected to conventional metallographic preparation with epoxy resin mounting, SiC sandpaper (220 to 4000 mesh) grinding, polishing with colloidal silica (13 nm) and etching in Kroll solution. The morphology of the powder particles and microstructures were analyzed in a scanning electron microscope (SEM). The chemical composition was verified by analyses in semi-quantitative way using energy dispersive spectroscopy - EDS. X-rays diffraction were determined in an equipment operating at 40 kV, 20 mA, range 20 ° - 80 ° and copper radiation (λ = 1,5418 Å). The measurements of Vickers microhardness (HV) was performed according to ASTM E384-11 using load of 0.3 kgf.

Results and discussion

The SEM micrographs of the morphology of these particles are shown in Fig. 1. The particles morphology of the TiH_2 (Fig. 1A) and NbH (Fig. 1B) are irregular-shaped rod-like with formation of sharp angles. The ZrH_2 (Fig. 1C) a sponge shaped, with a high surface roughness and aggregated particles and finally, metallic tantalum particles (Fig. 1D) is ligament-shaped [8].
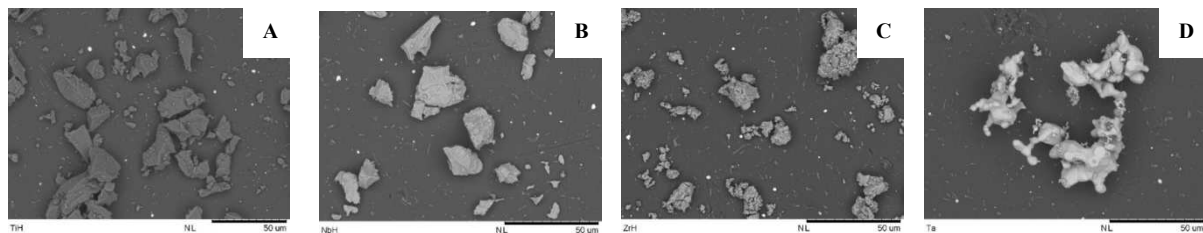

Fig. 1. Scanning electron micrographs of the starting powders. (A) TiH_2, irregular rod-like particles morphologies, (B) NbH, irregular rod-like particles morphologies, (C) ZrH, sponge particles morphologies, and (D) tantalum, ligamental particles morphology.

The starting materials were subjected to high-energy milling with mill speed of 200 rpm for 240 min for formation of the alloy Ti-8.5Nb-4.5Ta-13Zr. Fig. 2 show the particle size distribution and Tab. 1 summarizes distribution of these values. It can be seen a large distribution of particles concentration between 0.93 and 8.78 µm with similar values of the D50% and mean size particles.
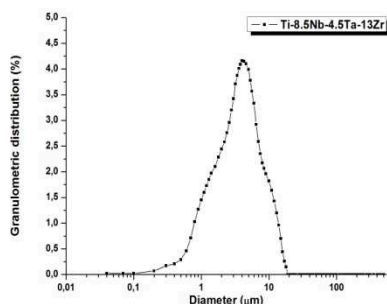

Fig. 2. Particle size distribution curve of Ti-8.5Nb-4.5Ta-13Zr alloy powder.

Table 1. Values of the distribution of particle sizes Ti-8.5Nb-4.5Ta-13Zr alloy powder.

D10% [µm]	0.9
D50% [µm]	3.4
D90% [µm]	8.8
Dmean% [µm]	4.2

The different morphology of the starting particles may have influenced these results shown in Tab. 1. The micrographs shown fragmented particles and in agglomerated shaped after the high-energy milling of alloy powder, see Fig. 3.
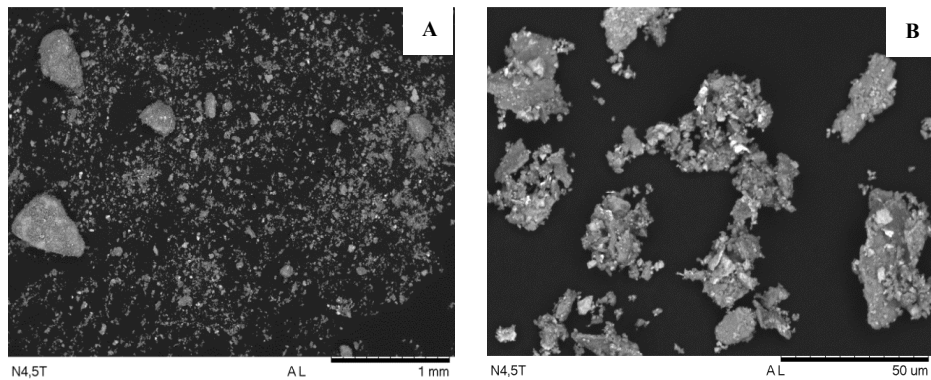

Fig. 3. Morphologies of the particles after high-energy milling as observed using scanning electron microscopy. (A) General appearance of the particles, (B) Agglomerated and aggregated particles with average size around 50 μm.

The Fig. 3 and the Table 1 reported here one can clearly observe that the mean particles size do not correspond with those shown in the micrographs, indicating agglomeration and particles aggregates of up to 50 μm. The large distribution of particles is due to the high energy milling process, which for this alloy system is classified as ductile-brittle [9], i.e., the hydrides corresponded to the fragile parts and metallic tantalum the ductile particles. The milling of ductile metallic powders becomes very difficult and may occur cold welding of the particles, decreasing grinding efficiency in the range from 1 % to 3 % [10].

The typical microstructures of the Ti-8.5Nb-4.5Ta-13Zr alloy as-sintered from the different cooling rates such furnace cooling (FC), air cooling (AC) and water quenching (WQ) are shown in Fig. 4. The general aspects of micrographs for specimens sintered at 1150 °C with furnace cooling, Fig. 4A, consists of dark and light regions which did not form solid solution in the sintering. The EDS semi-quantitative analysis of regions marked with the numbers (1), (2) and (3) in micrographs (Fig. 4A, Fig. 4C and Fig. 4E) indicate a compositions (% mass) of the these regions: (1) dark regions are predominantly titanium, (2) light regions essentially niobium and (3) high concentrations of titanium and niobium. The spot indicated by the number (2), shows that the irregular-shape of the niobium particles become rounded forming the microstructural appearance shoerd by point (3). It can be observed the presence of cracks and pores. The areas that concentrate larger particles and agglomerates are considered high-density points and the neighboring regions of low density. These differences between regions originate stress fields during sintering [11]. A similar behavior has been also observed for air cooling and water quenching, Fig. 4C and 4E.
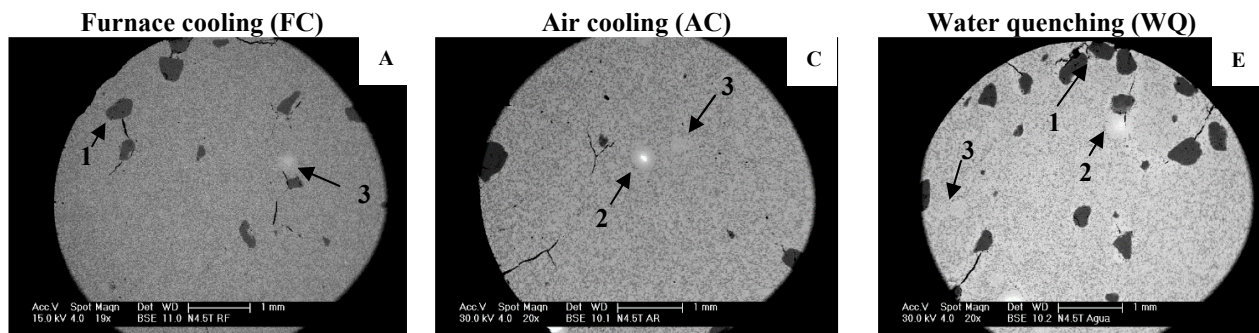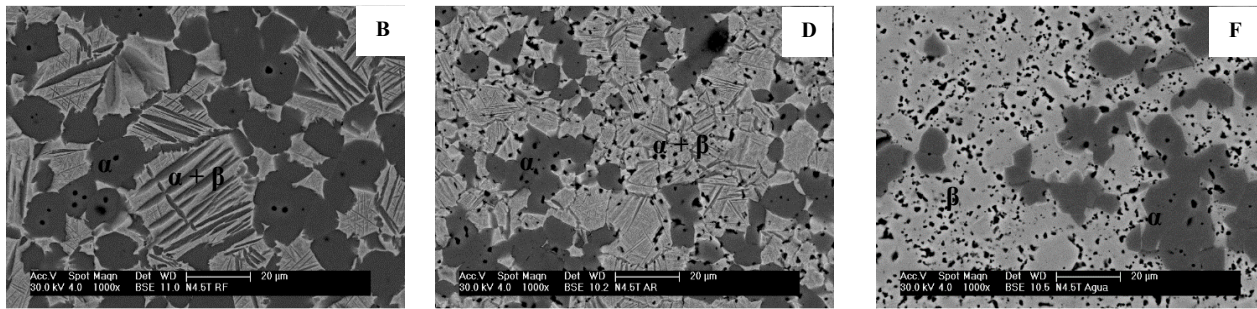
Fig. 4. SEM micrographs of the Ti-8.5Nb-4.5Ta-13Zr alloy as-sintered and after different cooling rates - furnace cooling (FC), air cooling (AC) and water quenching (WQ).

The microstructures of the alloy consists of β region (light gray) and α region (dark gray), Fig. 4B, Fig. 4D and Fig. 4F. The α-phase appears in two different structures: equiaxed grains and Widmanstätten structure, characterized in form of "needles or rods", being dispersed in the β-phase. The microstructural changes that occur from the β field are determined by the cooling rate of the alloy. During the sintering, alloy was inserted in the β-phase field and starting from a sufficiently slow cooling, for example as cooling furnace, will not change this field until the β-transus temperature (885 °C) be achieved. Below this, the transformation of β → α + β phase, which occurs in the growth and nucleation of α contours of the β grains. As the alloy is cooled, α may increase the grain boundary structure for changing the lamellar α grains, also known as α "colony" [12].

The Widmanstätten structure is more evident in the furnace and air cooled samples (Fig. B and Fig. D). The water quenching (Fig. 4F) was not displaying this structure, only α grains in β-matrix. The main factor for this difference in preferential formation of the structure is given by the variation of the diffusion coefficient (D) in a function of temperature (T). The values of the self-diffusion coefficient of titanium in the sintering temperature used in this study (1150 °C) are 2.35×10^{-13} $m^2.s^{-1}$ for Ti-β and 2.35×10^{-17} $m^2.s^{-1}$ for Ti-α, representing four orders of magnitude higher for Ti-β when compared to Ti-α [12].

Analysing the micrographs with air and water cooling (Fig. D and Fig. F) it can be observed that despite the sintering have occurred in the β-phase field, there are presence of β-stabilizers elements, the alloys still have α-phase contained in the β-matrix. The cooling rates for the conditions in air and in water are higher when compared with furnace cooling, it is suggested that there α-phase retention during the process of transformation of β → α + β (in air) and β → α (in water), since the diffusion coefficient of the Ti-α is less than β-Ti. The α-phase retention occur during the sintering time it was not completely diffused β in the matrix, due to wide particle size distribution and the presence of agglomerates which act as diffusion barriers. The difficulty of dissolving niobium in the β-matrix is mainly due to the low diffusion coefficient this element, about two orders of magnitude lower than the Ti-β [12].

The samples as-sintered presented high densification for the conditions of furnace and air cooling, 98 % of the theoretical density for both, however, the water quenching exhibit a decrease in density of about 96 %. It is suggested that the lower density in the alloy with water quenching is due to a greater amount of titanium and niobium regions, which did not form solid solution during sintering and to the heat treating condition with a higher cooling rate. Hence, these regions act as diffusion barriers, difficulting the achivement of final high density of the sample.

The Fig. 5 shows the X-ray diffractograms of Ti-8.5Nb-4.5Ta-13Zr alloy at different cooling rates - furnace cooling (FC), air cooling (AC) and water quenching (WQ). All the XRD patterns showed phases of Ti-α compact hexagonal structure and Ti-β of body-centered cubic structure. The alloys can be classified as α + β type. In the furnace cooling condition it is observed a greater intensity of the α-phase (~ 40° - the most intense peak) compared to β-phase (~ 38° - most intense peak), thus that increases the cooling rate, peak main intensity β-phase tends to increase, while the corresponding α-phase decrease.
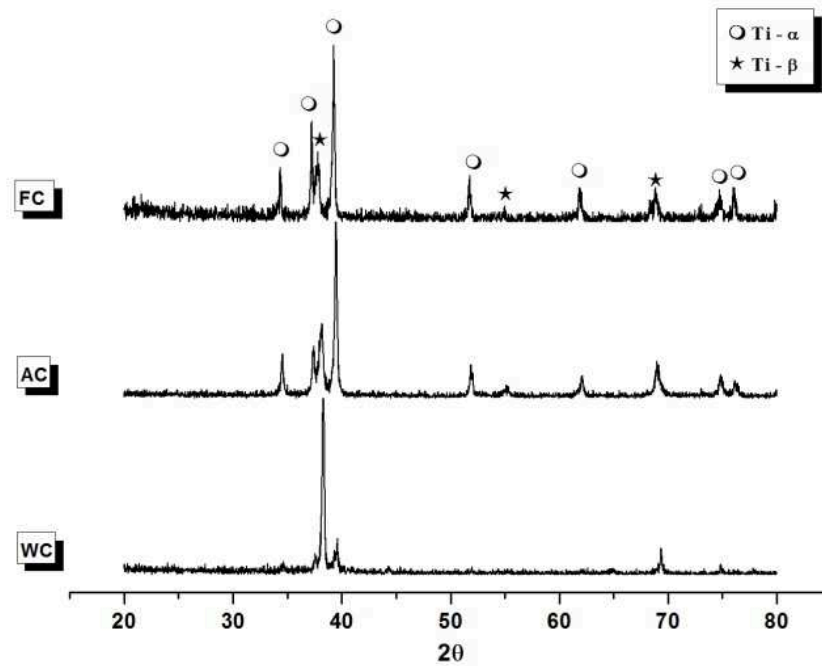
Fig. 5. X-ray diffractograms of the Ti-8.5Nb-4.5Ta-13Zr alloy as-sintered and after different cooling rates - furnace cooling (FC), air cooling (AC) and water quenching (WQ).

The as-sintered samples presented microhardness values around 554 ± 16 HV for furnace cooling and equivalence between the values obtained for cooling air and water quenching, 478 ± 10 HV and 471 ± 18 HV, respectively, as shown Fig. 6. It can be seen that the microhardness decreases with increasing rate cooling. It is known that the densification, grain sizes, structures and phases present can influence the mechanical property of hardness. As shown above, the cooling condition in the water show lower value of densification being in accordance with the hardness value. The retained α-phase produces an increase in the hardness of the titanium alloy [13] and has compact hexagonal structure having greater hardness compared to the β phase of body-centered cubic structure. The increase in hardness is due to higher HCP packing factor in compared to BCC, 0.74 and 0.68, respectively.
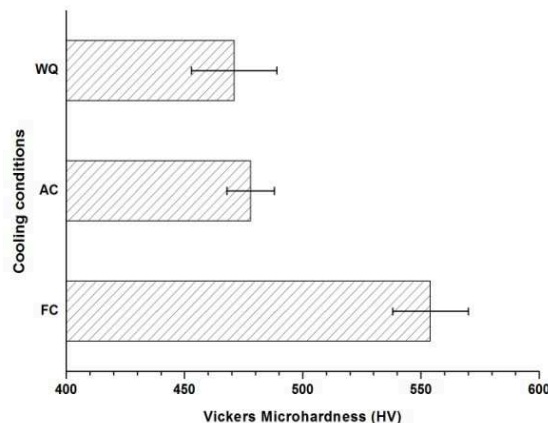

Fig. 6. Microhardness of the Ti-8.5Nb-4.5Ta-13Zr alloy as-sintered from the different cooling rates - furnace cooling (FC), air cooling (AC) and water quenching (WQ).

Conclusion

In the present study, the presence of brittle and ductile particles during the process of high-energy milling contributed to the formation of agglomerated and aggregated particles and that influence the final microstructure of the alloy. Due to the presence of titanium and niobium showing no complete solid solution in the microstructure, promoted product heterogeneity, and that

contributed to the propagation of cracks and pores in the grain boundaries. Besides, the final microstructure and mechanical properties hardness are too much influenced by the cooling conditions of the alloy and are formed by alpha and beta phases.

References

[1] Q. Chen, G.A. Thouas: Mater. Sci. and Eng. R Vol. 87 (2015), p. 1.

[2] M. Gheetha, A.K. Singh, R. Asokamani, A.K. Gogia: Prog. Mater. Sci. Vol. 54 (2009), p. 397.

[3] V. Brailovski, S. Prokoshkin, M. Gauthier, K. Inaekyan, S. Dubinskiy:. J. Alloys Compd. Vol. 577s (2013), p. s413.

[4] D. Zhao, K. Chang, T. Ebel, M. Qian, R. Willumeit, M. Yan, F. Pyczak: J. Mech. Behav. Biomed. Mater. Vol. 28 (2013), p. 171.

[5] D. Raducanu, E. Vasilescu, V.D. Cojocaru, I. Cinca, P. Drob, C. Vasilescu, S.I. Drob:J. Mech. Behav. Biomed. Mater. Vol. 4 (2011), p. 1421.

[6] P. Majumdar: Micron Vol. 43 (2012), p. 876.

[7] J.H. Duvaizem, N.M.F. Mendes, J.C.S. Casini, A.H. Bressiani, H. Takiishi: Mater. Sci. Forum Vol. 802 (2014), p. 457.

[8] R.M. German: *Powder Metallurgy Science*. (Princeton 2nd ed. New Jersey, 1994).

[9] L. Lü, M.O. Lai: *Mechanical Alloying*. (Norwell first ed. Massachusetts, 1998).

[10] C. Suryanarayana: Prog. Mater. Sci. Vol. 46 (2001), p. 1.

[11] F. Thümmler, R. Oberacker: *An Introduction to Powder Metallurgy*. (London, 1993).

[12] G. Lütjering, J.C. Williams: *Titanium*. (Second ed. Berlin, 2007).

[13] J. Málek, F. Hnilica, J. Veselý, B. Smola: Mater. Charact. Vol. 84 (2013), p. 225.